Deep spin-glass hysteresis-area collapse and scaling in the three-dimensional ±J Ising model

Citation: Sariyer, Ozan, Alkan Kabakcioglu, and A. Berker. "Deep Spin-glass Hysteresis-area Collapse and Scaling in the Three-dimensional ±J Ising Model." Physical Review E 86.4 (2012). © 2012 American Physical Society

As Published: http://dx.doi.org/10.1103/PhysRevE.86.041107

Publisher: American Physical Society

Persistent URL: http://hdl.handle.net/1721.1/75818

Version: Final published version: final published article, as it appeared in a journal, conference proceedings, or other formally published context

Deep spin-glass hysteresis-area collapse and scaling in the three-dimensional $\pm J$ Ising model

Ozan S. Sarıyer,[1] Alkan Kabakçıoğlu,[1] and A. Nihat Berker[2,3]
[1]*Department of Physics, Koç University, Sarıyer 34450, Istanbul, Turkey*
[2]*Faculty of Engineering and Natural Sciences, Sabancı University, Orhanlı, Tuzla 34956, Istanbul, Turkey*
[3]*Department of Physics, Massachusetts Institute of Technology, Cambridge, Massachusetts 02139, USA*
(Received 31 May 2012; published 5 October 2012)

We investigate the dissipative loss in the $\pm J$ Ising spin glass in three dimensions through the scaling of the hysteresis area, for a maximum magnetic field that is equal to the saturation field. We perform a systematic analysis for the whole range of the bond randomness as a function of the sweep rate by means of frustration-preserving hard-spin mean-field theory. Data collapse within the entirety of the spin-glass phase driven adiabatically (i.e., infinitely slow field variation) is found, revealing a power-law scaling of the hysteresis area as a function of the antiferromagnetic bond fraction and the temperature. Two dynamic regimes separated by a threshold frequency ω_c characterize the dependence on the sweep rate of the oscillating field. For $\omega < \omega_c$, the hysteresis area is equal to its value in the adiabatic limit $\omega = 0$, while for $\omega > \omega_c$ it increases with the frequency through another randomness-dependent power law.

DOI: 10.1103/PhysRevE.86.041107 PACS number(s): 05.70.Ln, 75.60.Ej, 64.60.Ht, 75.10.Nr

Hysteresis in magnetic materials has been a subject of interest for quite some time due to its applications in magnetic memory devices and as a testing ground for theories of nonequilibrium phenomena [1–4]. The hysteresis area which measures the magnetic energy loss in the material is connected with the Barkhausen noise [5,6] due to irreversible avalanche dynamics [7–12]. The existing literature on hysteresis in random magnets focuses mostly on random-field models [12–15] while numerical studies on random-bond models are mostly at zero temperature [16–22]. To our knowledge, there has been no finite-temperature study of the hysteresis loss, especially in the spin-glass phase where large avalanches are expected to be severely prohibited. We here investigate the adiabatic and dynamic hysteresis in the the $\pm J$ random-bond Ising spin glass [23] on a finite, three-dimensional simple cubic lattice with periodic boundary conditions. We show that the hysteresis area obeys a scaling relation in the whole spin-glass phase, in accord with earlier theoretical studies which observed scale invariance over the whole range about the critical disorder for various disorder-driven systems [15–17]. Moreover, this scaling data collapse is also observed for experimental systems over wide ranges of the temperature and the magnetic field: Gingras *et al.* observed a universal data collapse over four decades in a geometrically frustrated antiferromegnet $Y_2Mo_2O_7$ [24], while Gunnarsson *et al.* observed such a data collapse for the short-range Ising spin glass $Fe_{0.5}Mn_{0.5}TiO_3$ [25].

The $\pm J$ Ising spin-glass model is defined by the dimensionless Hamiltonian

$$-\beta\mathcal{H} = \sum_{\langle ij\rangle} J_{ij}s_i s_j + H\sum_i s_i \,, \tag{1}$$

where $\beta \equiv \frac{1}{k_B T}$ is the inverse temperature. The first sum in Eq. (1) is over the pairs of nearest-neighbor sites (i,j), where J_{ij} is the quenched-random local interaction between the classical Ising spins $s_i = \pm 1$. The probability distribution function for J_{ij} is given by

$$P(J_{ij}) = p\,\delta(J_{ij} + J) + (1-p)\delta(J_{ij} - J)\,. \tag{2}$$

H in the second term in Eq. (1) is the uniform external magnetic field. With a proper choice of units, the temperature for the system may be defined as $T \equiv 1/J$. A random distribution of the ferromagnetic and antiferromagnetic bonds gives rise to frustration and yields a spin-glass phase for a range of p values. Ising spin-glass models are widely used as a tool for understanding the properties of experimental spin glasses such as $Pr_{0.6}Ca_{0.4}Mn_{0.96}Ga_{0.04}O_3$ [11], $Fe_{0.5}Mn_{0.5}TiO_3$ [25–27], $LiHo_{0.167}Y_{0.833}F_4$ [28], and $Cu_{3-x}AlMn_x$ [29]. Without loss of generality we set $p \leqslant 0.5$ since the partition function is invariant under the transformation $p, \{s_i^A\}, \{s_j^B\} \to (1-p)$, $\{s_i^A\}, \{-s_j^B\}$, where A and B signify the two sublattices.

For small values of p and $H = 0$, the orientational (up-down) symmetry is spontaneously broken below a critical temperature $T_c(p)$ and long-range ferromagnetic order sets in. This phase is well understood within the Landau picture where the free energy landscape is described by two minima at magnetizations $\pm m(T,p)$. Beyond a critical fraction p_c of the antiferromagnetic bonds, reducing temperature drives the system into a glassy phase. The low-temperature phase now retains its orientational symmetry and a new, randomness-dominated phase which has a broken replica symmetry appears [30,31]. In this phase, the free energy landscape is rough, with many local minima at significantly nonoverlapping configurations. Meanwhile, the dynamics slows down to the extent that the relaxation time diverges [32]. At high temperatures $T > T_c(p)$, both ordered phases give way to a paramagnetic state where the entropic contribution to the free energy is dominant. While the critical temperature strongly depends on p along the ferromagnet-to-paramagnet phase boundary, only a weak dependence of T_c on p is observed for the spin-glass phase [32,33]. In this study, we investigate the hysteretic behavior of a spin glass under the uniform magnetic field H that is swept at a constant rate ω. A past computational study similar to ours [34] considered a time-dependent quenched-random magnetic field that was conjugate to the spin-glass order parameter.

We use hard-spin mean-field theory (HSMFT), a self-consistent field theoretical approach [34–50] that preserves the effects due to the frustration (crucial for the spin-glass

phase) generated by the randomly scattered antiferromagnetic bonds. HSMFT is defined by the refined set of self-consistent equations

$$m_i = \sum_{\{s_j\}} \left\{ \left[\prod_j P(m_j, s_j) \right] \tanh\left(\sum_j J_{ij} s_j + H \right) \right\} \quad (3)$$

for the local magnetization m_i at each site i, whose nearest neighbors are labeled by j. The single-site probability distribution is

$$P(m_j, s_j) = \frac{1 + m_j s_j}{2} . \quad (4)$$

The local magnetization m_i at site i satisfies $-1 \leqslant m_i \leqslant 1$. The hard-spin mean-field theory Eq. (3) has been discussed in detail by the authors of Refs. [34–50].

HSMFT has been successfully applied to spin glasses [34,43]. In this paper we make use of the method to investigate the scaling of the hysteresis area under a uniform, time-dependent magnetic field. To this end, we consider a $20 \times 20 \times 20$ cubic lattice with periodic boundary conditions. We have checked in this study and in a previous study [34] that our hard-spin mean-field theory results are independent of size for an $L \times L \times L$ system for $L \gtrsim 15$. A particular realization at a given (T, p) is generated by the assignment of the quenched-random coupling constants J_{ij} according to the probability distribution of Eq. (2) and, initially, a random and unbiased choice of spins $s_i = \pm 1$. To determine the hysteresis curves, the system is first saturated by a sufficiently large external field H_s, the minimum value of H for which Eq. (3) yields an average magnetization $m = (1/L^3) \sum_i m_i = 1$ within an accuracy $\epsilon_m \equiv 10^{-6}$. Then, the path $H_s \to -H_s \to H_s$ is traversed with steps $\Delta H = H_s/100$ or smaller. For each incremental change of the field, the system is allowed to relax a number of time steps $\tau = 1/\omega$. A time step corresponds to successive iterations of Eq. (3) on L^3 arbitrarily chosen sites. An infinitely slow sweep is obtained as the limit $\tau \to t_R$, where the HSMF equations converge to a self-consistent solution within the tolerance interval ϵ_m. Thus, t_R is the relaxation time of the system.

The infinitely slow-sweep hysteresis curves obtained in the ferromagnetic and spin-glass phases are shown in Fig. 1. The usual jump in the magnetization at a coercive field H_c, observed for small p, is associated with a system-wide avalanche in the ferromagnetic phase. For p larger than a critical value p_c, this picture is replaced by a slanted hysteresis curve and a smaller hysteresis area, typical of spin-glass materials [3,11,29]. This converse hysteretic behavior, associated with the Barkhausen noise [5,6], is a consequence of the power-law distribution of avalanches which is well established [6,7,10–12,14–18,20,21,29,51] for several frustrated systems with quenched disorder. The hysteresis area disappears in the paramagnetic phase.

In Fig. 2, we present the infinitely slow-sweep hysteresis area globally, for all temperatures and antiferromagnetic bond probabilities, on a logarithmic color-contour plot. The hysteresis area A_0 vanishes in the region shown in dark blue, which corresponds to the paramagnetic phase, while it is nonzero in the ferromagnetic and spin-glass phases, respectively, on the left and right of the lower half of Fig. 2.

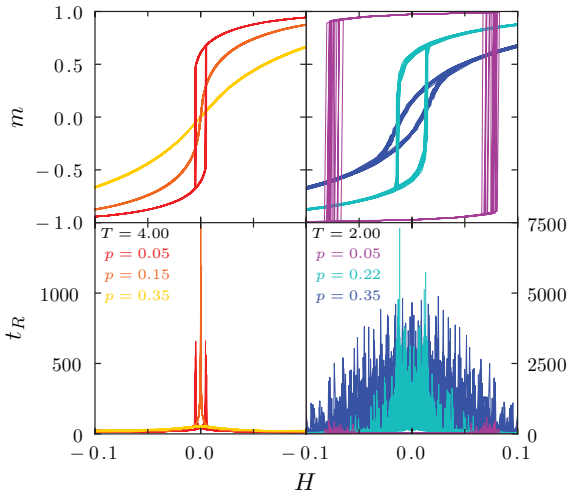

FIG. 1. (Color online) Hysteresis curves (upper) and relaxation times (lower) at high ($T = 4.00$, left) and low ($T = 2.00$, right) temperatures. Data are for p values either deep in the ferromagnetic ($p = 0.05$), spin-glass ($T = 2.00$, $p = 0.35$), or paramagnetic ($T = 4.00$, $p = 0.35$) phases, or close to the phase boundaries for the ferromagnetic-paramagnetic ($T = 4.00$, $p = 0.15$) or ferromagnetic-spin-glass ($T = 2.00$, $p = 0.22$) transitions. For each case, an overlay of 20 distinct runs with different random-bond arrangements is shown.

The para-ferro and para-spin-glass phase boundaries are easily determined by locating the temperature at which A_0 vanishes (i.e., falls below ϵ_m). A set of p scans for different temperatures and a set of temperature scans for various p values are given in Fig. 3. The low-temperature ferro-spin-glass boundary is located at $p_c \simeq 0.22$ and is calculated as the inflection point for the maximum slope of the hysteresis curve as a function of antiferromagnetic bond probability [16]. The phase boundaries are consistent with the well-known phase diagram for the three-dimensional $\pm J$ model [33] and in fair comparison with

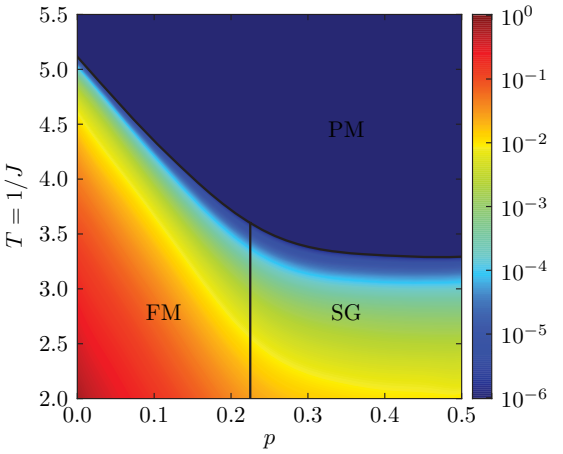

FIG. 2. (Color online) Logarithmic contour plot of the infinitely slow-sweep hysteresis area A_0 as a function of antiferromagnetic bond probability p and temperature $T = 1/J$. The thick vertical line denotes the phase boundary between the ferromagnetic and the spin-glass phases as described in the text, while the other thick line bounds the paramagnetic phase where the infinitely slow-sweep hysteresis area is less than the precision used in the consistent-field calculations (i.e., $A_0 < 10^{-6}$).

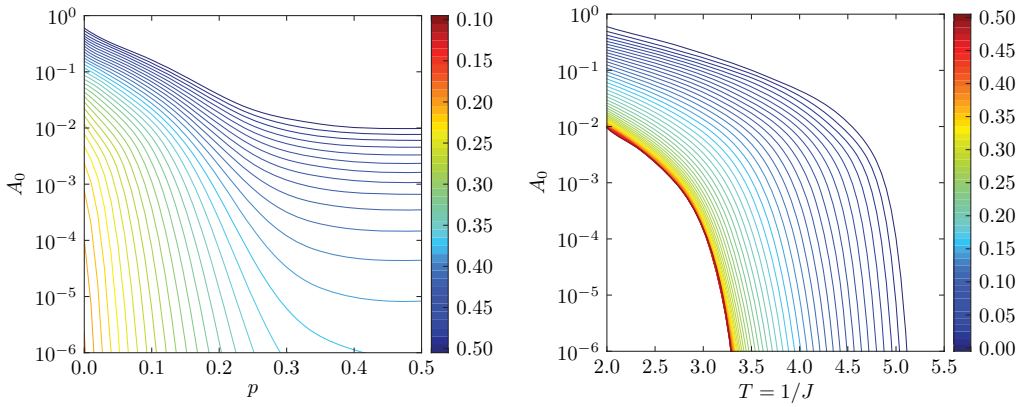

FIG. 3. (Color online) Infinitely slow-sweep hysteresis area A_0, as a function of antiferromagnetic bond probability p for temperatures (indicated in the color legend) $1/T = J = 0.10, 0.11, \ldots, 0.50$ (left) and as a function of temperature $T = 1/J$ for antiferromagnetic bond probabilities (indicated in the color legend) $p = 0.00, 0.01, \ldots, 0.50$ (right). Each curve is a tenth degree polynomial fit to the averages over 20 realizations.

the experimental temperature-concentration phase diagrams of the various $Eu_xSr_{1-x}S_ySe_{1-y}$, solid $(o\text{-}H_2)_{1-x}(p\text{-}H_2)_x$, and AuFe systems reviewed in Ref. [32].

We here focus on the scaling form of the hysteresis area in the spin-glass phase and show that a unique scaling-function governs the whole range of p and J within the spin-glass phase. To this end, we first express the hysteresis area in the form $A_0 = A_0(\tilde{p}, \tilde{J})$, where $\tilde{p} \equiv \frac{p-p_c}{p_c}$ and $\tilde{J} \equiv \frac{J-J_c}{J_c}$ are the reduced displacements from phase boundaries. We then postulate the multivariate scaling form

$$A_0(\tilde{p}, \tilde{J}) = \lambda^c A_0(\lambda^a \tilde{p}, \lambda^b \tilde{J}) , \tag{5}$$

which by letting $\lambda = \tilde{p}^{-1/a}$ reduces to

$$A_0(\tilde{p}, \tilde{J}) = \tilde{p}^{-c/a} A_0(1, \tilde{p}^{-b/a} \tilde{J}) , \tag{6}$$

Defining $\nu \equiv c/a$, $\mu \equiv -b/a$, and $f(x) \equiv A_0(1,x)$, we obtain

$$\tilde{p}^{\nu} A_0(\tilde{p}, \tilde{J}) = f(\tilde{p}^{\mu} \tilde{J}) . \tag{7}$$

The sought collapse is obtained by the choice of scaling exponents $\mu = 1$ and $\nu = 2$. The data shown in Fig. 3 collapse onto a single curve shown in Fig. 4, where the left-hand side (LHS) of Eq. (7) is plotted against the argument on the right-hand side (RHS) for 28 evenly spaced values of p above p_c. The origin corresponds to the phase boundary between the spin-glass and paramagnetic phases. The log-log plot of the same collapse shown in the inset of Fig. 4 suggests that the scaling function has the form $f(x) \propto x^{1.72}$, yielding a hysteresis area $A_0 \propto \tilde{p}^{\alpha} \tilde{J}^{\beta}$ with $\alpha \simeq -0.28$ and $\beta \simeq 1.72$. Interestingly, unlike the case of the usual critical phenomena, the scale-invariance applies to the entire spin-glass phase and not just to the vicinity of the critical phase boundary.

Having analyzed the limit with infinitely slow-sweep rate, we next consider the dynamic hysteretic response as a function of the magnetic field frequency. One can simulate the finite oscillation frequency by iterating Eq. (3) for a predetermined number of steps t, instead of waiting until a steady state is reached. The sweep rate $\omega = 1/t$ is proportional to the frequency of the applied field up to a material-dependent spin relaxation time. The hysteresis area $A(\omega, p, J)$ deviates from the value at infinitely slow sweep $A_0 = A(\omega = 0, p, J)$ and increases with increasing sweep rate ω. This can be understood by observing that the slow response of the magnetization to a time-varying field inflates the hysteresis curve along the field direction. The typical behavior observed in various experimental and theoretical magnets (typically pure magnets or random-field systems) [52–56] is

$$A(\omega, p, J) = A_0 + g(p, J)\, \omega^b , \tag{8}$$

where b is the sweep-rate exponent. We investigate whether the random-bond Ising spin glass obeys a similar scaling relation.

A typical scan of the hysteresis area as a function of ω displays two dynamic regimes, separated by a critical sweep

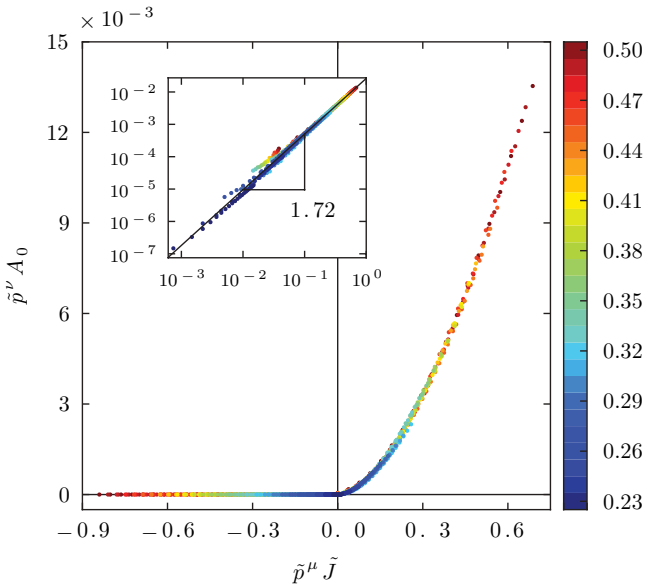

FIG. 4. (Color online) Scaling of the hysteresis area in the spin-glass phase as a function of reduced antiferromagnetic bond concentration $\tilde{p}$ and the reduced bond strength $\tilde{J}$, for various p values as shown in the color legend. The scaling function $f(x)$ given by the RHS of Eq. (7) on which all data points collapse is consistent with a same power law within the entire spin-glass phase.

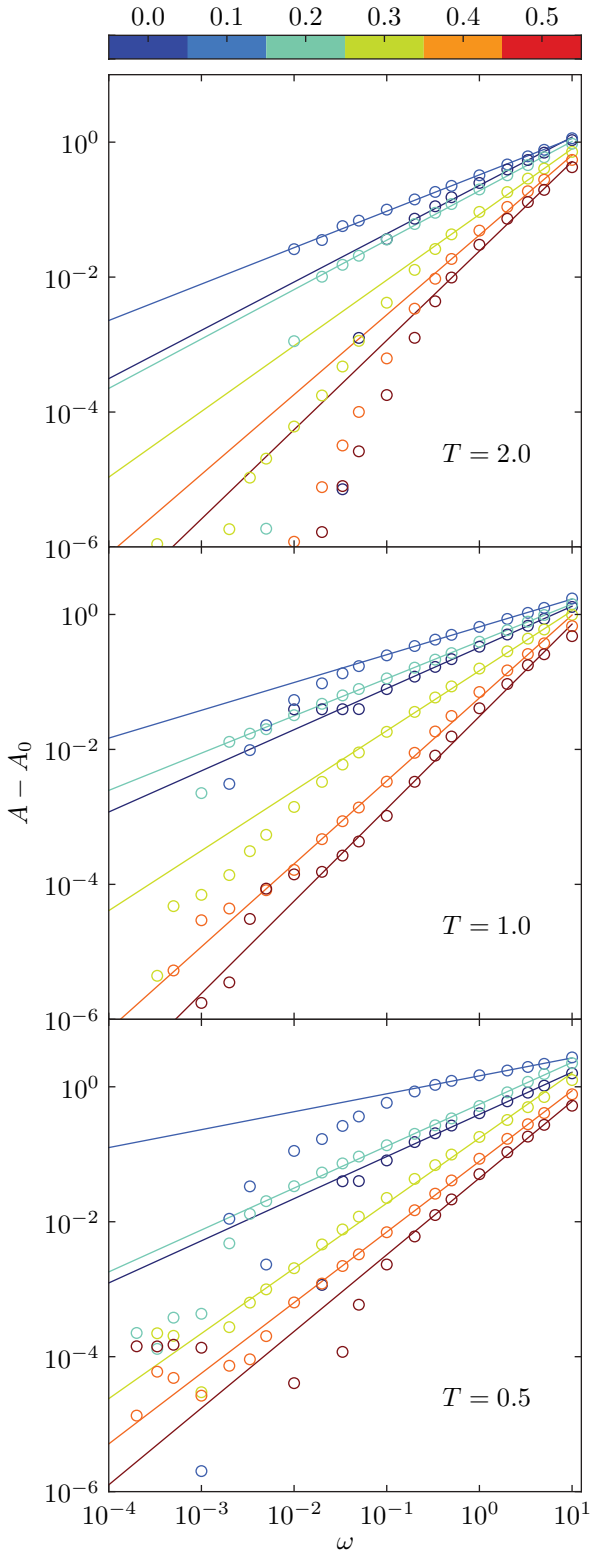

FIG. 5. (Color online) Hysteresis area difference $A - A_0$ versus sweep rate ω, for temperatures $T = 2.0$, 1.0, 0.5 from top to bottom and for antiferromagnetic bond fractions $p = 0.0$, 0.1, ...,0.5 as shown in the color legend.

rate ω_c that depends on p, J, and the system size (Fig. 5). For a sufficiently slowly varying field $\omega < \omega_c$, the area is pinned at the value A_0. In this regime, the avalanches that are triggered

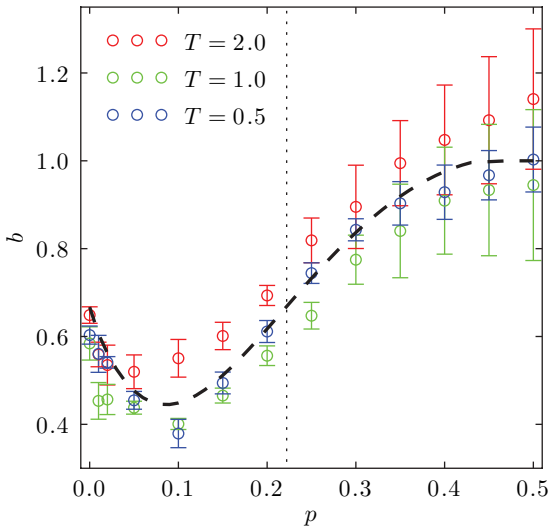

FIG. 6. (Color online) Sweep-rate exponent b versus antiferromagnetic bond fraction p for temperatures $T = 2.0$, 1.0, and 0.5. The dashed curve depicts the general trend of the sweep-rate exponent, while the dotted vertical line marks the phase transition from ferromagnetic to spin-glass phase.

by an incremental increase in the field decay within a period $1/\omega$ or smaller. For faster sweeps ($\omega > \omega_c$), the increase in the area follows the power law in Eq. (8), with a p-dependent exponent b. In the ferromagnetic phase with weak disorder, the two dynamic regimes are separated by a sharp increase in the hysteresis area. This transition gets significantly smoother in the spin-glass phase, especially far from the ferromagnetic-spin-glass boundary. For larger systems, one expects ω_c to recede and the power-law behavior to dominate.

Figure 6 shows the sweep-rate exponent b calculated as a function of the antiferromagnetic bond fraction p, at fixed temperatures $T = 1/J = 2.0$, 1.0, and 0.5. The hysteresis area is calculated for the sweep rates $\omega = 1, 0.5, 0.\bar{3}, 0.2, 10^{-1}, \ldots, 10^{-4}$ at each p value, after averaging over ten realizations. The exponent values are obtained through fits to the data in the regime $\omega > \omega_c$ (typically two decades or more), using the functional form of Eq. (8). The error bars reflect only the scatter of the data relative to the fit. In the ferromagnetic phase $p < p_c$, we note that the calculated sweep-rate exponents lie in an interval of fairly good agreement with the various values obtained previously at $p = 0$, namely $b = 2/3$ [52–55] and $b = 0.52 \pm 0.04$ [53] from mean-field theory, $b = 0.61$ [53] from Glauber dynamics simulations, $b = 0.495 \pm 0.005$ [54] and $b = 0.45$ [56] from Monte Carlo simulations.

In conclusion, we have considered here the $\pm J$ Ising model under a uniform external field and investigated the scaling behavior of the saturation hysteresis area (i.e., far from the weak-field limit). We observed that the phase diagram can be derived from the hysteresis area alone and the ferromagnetic-spin-glass phase boundary corresponds to the inflection point with regard to bond-randomness strength p. When adiabatically driven, the area displays a data collapse within the entire spin-glass phase for all temperatures and p. The scaling function itself has a power-law form and the scale invariance extends far from the phase boundary, deep into the spin-glass phase.

The dynamical response under a fluctuating external field is also interesting. We find that, beyond a threshold value ω_c, the hysteresis area increases as a function of the field-sweep rate ω with a nonuniversal power law. This behavior is not limited to the vicinity of the phase transition. The associated exponent is found to be a function the randomness strength p. Moreover, this function is independent of temperature. In the limit of a pure magnet ($p \to 0$), we observe good agreement with the existing literature, despite the fact that the earlier theoretical work applied to a weak driving field, while we here consider sweeps across saturation limits. Figure 6 suggests that, relative to the ferromagnetic phase, the spin glass displays an amplified sensitivity to the field-sweep rate, again running in apparent contrast to the general wisdom that the hysteretic effects are suppressed within a spin glass. In fact, we note that the increase in the hysteresis area with ω is due to the magnet's delayed response to the changing field, and a signature of the spin-glass phase is the slowing down of precisely such relaxation phenomena.

ACKNOWLEDGMENTS

Support by the Alexander von Humboldt Foundation, the Scientific and Technological Research Council of Turkey (TÜBİTAK), and the Academy of Sciences of Turkey (TÜBA) is gratefully acknowledged. We acknowledge the hospitality of the TÜBİTAK-Bosphorus University Feza Gürsey Institute for Fundemental Sciences, for the computational support from the Gilgamesh cluster.

[1] G. Bertotti, *Hysteresis in Magnetism: for Physicists, Materials Scientists, and Engineers* (Academic, Amsterdam, 1998).
[2] F. Colaiori, Adv. Phys. **57**, 287 (2008).
[3] M. S. Pierce, C. R. Buechler, L. B. Sorensen, S. D. Kevan, E. A. Jagla, J. M. Deutsch, T. Mai, O. Narayan, J. E. Davies, K. Liu, G. T. Zimanyi, H. G. Katzgraber, O. Hellwig, E. E. Fullerton, P. Fischer, and J. B. Kortright, Phys. Rev. B **75**, 144406 (2007).
[4] H. G. Katzgraber and G. T. Zimanyi, Phys. Rev. B **74**, 020405(R) (2006).
[5] H. Barkhausen, Physik Zeits **20**, 401 (1919).
[6] G. Durin and S. Zapperi, in *The Science of Hysteresis*, edited by G. Bertotti and I. D. Mayergoyz, Vol. 2 (Academic, Amsterdam, 2005), p. 181.
[7] P. Bak, C. Tang, and K. Wiesenfeld, Phys. Rev. Lett. **59**, 381 (1987).
[8] P. J. Cote and L. V. Meisel, Phys. Rev. Lett. **67**, 1334 (1991).
[9] L. P. Lévy, J. Phys. I (Paris) **3**, 533 (1993).
[10] J. P. Sethna, K. Dahmen, S. Kartha, J. A. Krumhansl, B. W. Roberts, and J. D. Shore, Phys. Rev. Lett. **70**, 3347 (1993).
[11] V. Hardy, S. Majumdar, M. R. Lees, D. McK. Paul, C. Yaicle, and M. Hervieu, Phys. Rev. B **70**, 104423 (2004).
[12] O. Perković, K. Dahmen, and J. P. Sethna, Phys. Rev. Lett. **75**, 4528 (1995); O. Perković, K. A. Dahmen, and J. P. Sethna, Phys. Rev. B **59**, 6106 (1999).
[13] S. Sabhapandit, P. Shukla, and D. Dhar, J. Stat. Phys. **98**, 103 (2000).
[14] K. A. Dahmen, J. P. Sethna, M. C. Kuntz, and O. Perković, J. Magn. Magn. Mater. **226**, 1287 (2001).
[15] J. P. Sethna, K. A. Dahmen, and O. Perković, in *The Science of Hysteresis*, edited by G. Bertotti and I. D. Mayergoyz, Vol. 2 (Academic, Amsterdam, 2005), p. 107.
[16] E. Vives and A. Planes, Phys. Rev. B **50**, 3839 (1994).
[17] E. Vives, J. Goicoechea, J. Ortín, and A. Planes, Phys. Rev. E **52**, R5 (1995).
[18] E. Vives and A. Planes, J. Phys. IV (Paris) **5**, C2-65 (1995).
[19] A. K. Hartmann, Phys. Rev. B **59**, 3617 (1999).
[20] E. Vives and A. Planes, J. Magn. Magn. Mater. **221**, 164 (2000).
[21] F. Pázmándi, G. Zaránd, and G. T. Zimányi, Physica B **275**, 209 (2000).
[22] H. G. Katzgraber, F. Pázmándi, C. R. Pike, K. Liu, R. T. Scalettar, K. L. Verosub, and G. T. Zimányi, Phys. Rev. Lett. **89**, 257202 (2002).
[23] G. Toulouse, Commun. Phys.**2**, 115 (1977), reprinted in *Spin Glass Theory and Beyond*, edited by M. Mezard, G. Parisi, and M. A. Virasoro (World Scientific, Singapore, 1987), pp. 99–103.
[24] M. J. P. Gingras, C. V. Stager, N. P. Raju, B. D. Gaulin, and J. E. Greedan, Phys. Rev. Lett. **78**, 947 (1997).
[25] K. Gunnarsson, P. Svedlindh, P. Nordblad, L. Lundgren, H. Aruga, and A. Ito, Phys. Rev. B **43**, 8199 (1991).
[26] H. G. Katzgraber, D. Hérisson, M. Östh, P. Nordblad, A. Ito, and H. A. Katori, Phys. Rev. B **76**, 092408 (2007).
[27] A. Ito, H. Aruga, E. Torikai, M. Kikuchi, Y. Syono, and H. Takei, Phys. Rev. Lett. **57**, 483 (1986).
[28] W. Wu, D. Bitko, T. F. Rosenbaum, and G. Aeppli, Phys. Rev. Lett. **71**, 1919 (1993).
[29] E. Vives, E. Obradó, and A. Planes, Physica B **275**, 45 (2000).
[30] G. Parisi, Phys. Rev. Lett. **50**, 1946 (1983).
[31] M. Mézard, G. Parisi, N. Sourlas, G. Toulouse, and M. Virasoro, J. Phys. (Paris) **45**, 843 (1984); Phys. Rev. Lett. **52**, 1156 (1984).
[32] K. Binder and A. P. Young, Rev. Mod. Phys. **58**, 801 (1986).
[33] Y. Ozeki and H. Nishimori, J. Phys. Soc. Jpn. **56**, 1568 (1987).
[34] B. Yücesoy and A. N. Berker, Phys. Rev. B **76**, 014417 (2007).
[35] R. R. Netz and A. N. Berker, Phys. Rev. Lett. **66**, 377 (1991).
[36] R. R. Netz and A. N. Berker, J. Appl. Phys. **70**, 6074 (1991).
[37] J. R. Banavar, M. Cieplak, and A. Maritan, Phys. Rev. Lett. **67**, 1807 (1991).
[38] R. R. Netz and A. N. Berker, Phys. Rev. Lett. **67**, 1808 (1991).
[39] R. R. Netz, Phys. Rev. B **46**, 1209 (1992).
[40] R. R. Netz, Phys. Rev. B **48**, 16113 (1993).
[41] A. N. Berker, A. Kabakçıoğlu, R. R. Netz, and M. C. Yalabık, Turk. J. Phys. **18**, 354 (1994).
[42] A. Kabakçıoğlu, A. N. Berker, and M. C. Yalabık, Phys. Rev. E **49**, 2680 (1994).
[43] E. A. Ames and S. R. McKay, J. Appl. Phys. **76**, 6197 (1994).
[44] G. B. Akgüç and M. Cemal Yalabık, Phys. Rev. E **51**, 2636 (1995).
[45] J. E. Tesiero and S. R. McKay, J. Appl. Phys. **79**, 6146 (1996).
[46] J. L. Monroe, Phys. Lett. A **230**, 111 (1997).

[47] A. Pelizzola and M. Pretti, Phys. Rev. B **60**, 10134 (1999).
[48] A. Kabakçıoğlu, Phys. Rev. E **61**, 3366 (2000).
[49] H. Kaya and A. N. Berker, Phys. Rev. E **62**, R1469 (2000); also see M. D. Robinson, D. P. Feldman, and S. R. McKay, Chaos **21**, 037114 (2011).
[50] T. Çağlar and A. N. Berker, Phys. Rev. E **84**, 051129 (2011).
[51] E. Vives and A. Planes, Phys. Rev. B **63**, 134431 (2001).
[52] P. Jung, G. Gray, R. Roy, and P. Mandel, Phys. Rev. Lett. **65**, 1873 (1990).
[53] G. P. Zheng and J. X. Zhang, J. Phys.: Condens. Matter **10**, 1863 (1998).
[54] G. P. Zheng and J. X. Zhang, Phys. Rev. E **58**, R1187 (1998).
[55] G. P. Zheng and M. Li, Phys. Rev. B **66**, 054406 (2002).
[56] M. Acharyya and B. K. Chakrabarti, Phys. Rev. B **52**, 6550 (1995).